Targeting the Motor Protein Cagβ Blocks Oncoprotein CagA-induced Host Inflammation in *Helicobacter pylori:* An *in silico* Analysis

Shubhangi Majumder[1], Sanjib Das[2]*, Amalesh Mondal[2,3], Tanima Saha[2]*

[1]Department of Bioscience, JIS University

[2]Department of Molecular Biology and Biotechnology, University of Kalyani

[3]Department of Physiology, Katwa College, Katwa, Purba Bardhaman, West Bengal, 713130, India

***Corresponding Author**

DOI: https://doi.org/10.51244/IJRSI.2026.1307000394

Received: 07 August 2026; Accepted: 13 August 2026; Published: 20 August 2026

ABSTRACT

Helicobacter pylori is a common gut microbiota, responsible for severe gastritis, peptic ulcer disease and an increased risk of gastric cancer. The Cag pathogenicity island helps *H. pylori* cause disease by forming a molecular syringe to attack host cells that transfer the CagA oncoprotein into the gastric cells. Once inside the host cell, Cag A modifies multiple signalling pathways, leading to major alterations and even malignancy. Cagβ, the coupling protein of T4SS, plays a significant role in detecting and carrying CagA through an ATP-dependent mechanism. As Cagβ functions like a molecular motor of the secretion system, targeting this particular protein may provide a way to prevent CagA delivery. This study aims to model the 3D structure of Cagβ motor protein and identify repurposed drugs capable of inhibiting its activity through molecular docking studies. Venetoclax was found one of the most promising drug, having binding affinity of -11.6 Kcal/mol with expected structural stability via interaction with SER301, MET297, GLY309 and LEU249 residue. Blocking Cagβ regulated activity may block the CagA delivery into host cells, subsequently reducing downstream inflammatory signalling pathways and limiting the further pathogenesis of *H. pylori* infection.

Keyword: *Helicobacter pylori*, Cagβ, Cag A, Type IV Secretion System (or T4SS), Molecular docking, Drug repurposing.

INTRODUCTION

Helicobacter pylori selectively adapts itself to survive in the gastric mucosa in the human stomach. It has a helical shaped feature with multiple flagella that helps the bacterium to invade inside the protective host mucosal layer, allowing successful settlement for long term persistence in the extreme gastric surrounding (IARC). It globally infects over 50% of the world's population exceeding 80% in several developing nations (Guevara and Cogdill). While many individuals do not show any symptoms, thus long-term infection cause severe peptic ulceration (10-14%), gastric adenocarcinoma (1-3%) and deadliest, the gastric cancer which is responsible for over 750,000 deaths each year (Hooi et al.; Sung et al.) Because of its unique virulence characteristics and its established role in gastric cancer development, the World Health Organization (WHO) has classified *H. pylori* as a Group I carcinogen (Correa and Houghton). The effect of *H. pylori* is highly dependent on its pathogenic factors, in the middle of which the cytotoxin-associated gene pathogenicity island (CagPAI) plays a crucial role. The CagPAI encodes the Cag type IV secretion system (Cag-T4SS), a unique

ISSN No. 2321-2705 | DOI: 10.51244/IJRSI |Volume XIII Issue VII July 2026

protein that carries the CagA effector protein into the gastric cells. These further excite the production of proinflammatory cytokines, and eventually lead to damage of epithelial cells and gastric carcinogenesis (Tegtmeyer et al.; Tohidpour). A vital component of cag-T4SS is Cagβ, that is recognised as the molecular motor of the secretion system. Cagβ identifies the CagA substrate and utilizes the ATP hydrolysis to convey CagA via the secretion machinery into the host cells. As Cagβ is a key player in the process of CagA translocation, inhibiting the ATP-dependent activity can act as barrier to CagA and eventually halt the whole process. Therefore, Cagβ may be a probable drug targeting candidate that can suppress *H. pylori*- induced inflammation, thereby forms a powerful alternative to conventional antibiotic therapy (Wu et al.). In the current study, an *in-silico* approach including homology modelling, structural validation, binding site prediction, drug repurposing and molecular docking was applied to find the drugs capable for interacting with Cagβ which can subsequently interfere with CagA translocation, finally reducing the inflammatory responses of *H. pylori*.

METHODOLOGY

Protein sequence retrieval

Cagβ amino acid sequence of *H. pylori* strain ATCC700392/26695 was secured from the Uniport database (Bateman et al.). Uniport is one of the most standardised, widely and expertly curated protein database in the world. The obtained sequence was then used for the 3D structural modelling.

Homology modelling

As the crystal structure of Cagβ is unavailable, so 3D model was generated using SWISS-MODEL SERVER (Waterhouse et al.). It displayed different types of models based on the sequence query coverage; it is defined as the percentage of successful mapped sequences and built into a 3D model using a known template. A high coverage indicates maximum of the amino acid sequences are modelled (>80%) (Waterhouse et al.). Global model quality estimation (GMQE), score closest to 1, is considered the 'best model' as it reflects the overall reliability of the model (>0.70) (Waterhouse et al.). QMEAN Z-score is a statistical metric that compares the geometric features of the generated model with other thousands of experimental structures from protein data bank. The best score is considered between 0.0 to -2.0 (Benkert et al.).

Structural validation

The predicted structure is then evaluated using SAVES v6.0 (https://saves.mbi.ucla.edu), which is the structural analysis and verification server giving results based on parameters like- ERRAT; it is the analysis used to evaluate the model's atomic environment quality. Well refined structure is often 85-100% in score (Colovos and Yeates). Verify 3D measures how the model fits in its own amino acid sequences. To pass verify 3D, it requires at least 80% of the amino acids must score >0.1(Bowie et al.). More the green boxes, more better are the geometric values (Hooft et al.). PROCHECK, one of the most important parameters provides the most significant benchmark, the Ramachandran Plot. Ramachandran plot is classified into 4 quadrants, and the residues are plotted in 4 different coloured zones, flavoured regions (red), allowed regions (brown), generously allowed (yellow) and disallowed (white) (Ramachandran et al.). Another validation was done using ProSA server (Wiederstein and Sippl). It showed the overall model quality and local model quality based on Z-score and plot residue score. The Z-score measures how many standard deviations the energy of the generated model is away from the mean energy of a large database of native, high-resolution protein structures determined by X-ray crystallography or NMR spectroscopy. More the negative Z-score, more the stable and relaxed conformation (Wiederstein and Sippl). In the plot residue scores, the residue plot graph shows the status of every amino acid along the sequence. An increased negative value is preferable, while, a positive value indicates poor result(Wiederstein and Sippl).

Binding site prediction

After a strong validation, the 3D model of Cagβ needs ligand binding pockets, which was identified using DrugRep server (Gan et al.). A receptor-based screening was done, which guided a cavity-detection and

ISSN No. 2321-2705 | DOI: 10.51244/IJRSI |Volume XIII Issue VII July 2026

docking pockets of protein receptors. Firstly the predicted binding pockets are given based on their volume, centre and size, then the binding pocket was selected on the basis of amino acid domain.

Molecular docking

Molecular docking is a computer-based method used to study how drug molecules interact with target Cagβ at the atomic level. This helps to analyse the chemical behaviour of the drug within a protein's specific binding pocket. The process firstly predicts the shape, position and pose of the drug molecule inside the binding site; secondly it calculates how powerful is the ligand attaching itself to the protein. In this study, AutoDock Vina-1.5.6 is used to identify how the drug will fit and position inside the target binding site (Oleg and Arthur J.). AutoDock Tools contain a 3D search area called grid box with the grid point spacing, and box dimension of 30*30*30, centred at the exact coordinates X,Y and Z in -9.3, -1.6, 4.7, respectively. After the protein was prepared accordingly, the drug or the ligand was then torsion-tree defined to allow for molecular flexibility during the interaction.

Visualization

For the visualization, the results are seen in PyMOL (3.1.8), as it provides a clear view of the drug ligand and the protein interaction at the atomic level (DeLano). This enables visual evaluation of whether the drug is properly positioned within the target binding site. By measuring the bond distances in Ångström (Å), we were able to assess the interactions, as shorter bond lengths within the optimal hydrogen-bonding ranges indicate a more stable and energetically favourable complex (Bissantz et al.). Accordingly, the best drug was selected for the stable binding with Cagβ.

RESULTS

Protein modelling and validation

The 3D structure of the Cagβ protein was modelled using SWISS-MODEL server, selecting the best drug, based on the GMQE score and template match (Fig. 1). As the template shared more than 50% similarity, the model was suitable for drug studies. The coverage of this protein was 100%, QMEAN Z-score is -1.2. The validation confirmed high structural quality, the verify3D scored 87% of green boxes, the Ramachandran plot analysis placed 89.9% of residues in the most favoured regions and 7.6% in allowed regions, with only 1.9% in disallowed region. A ProSA Z- score of -10.34 and an overall negative energy plot showed a stable structure. Further the ERRAT score of 89.53 resulted non-atomic interactions. Together, these confirmed that the Cagβ model was reliable for further studies (Fig. 2).

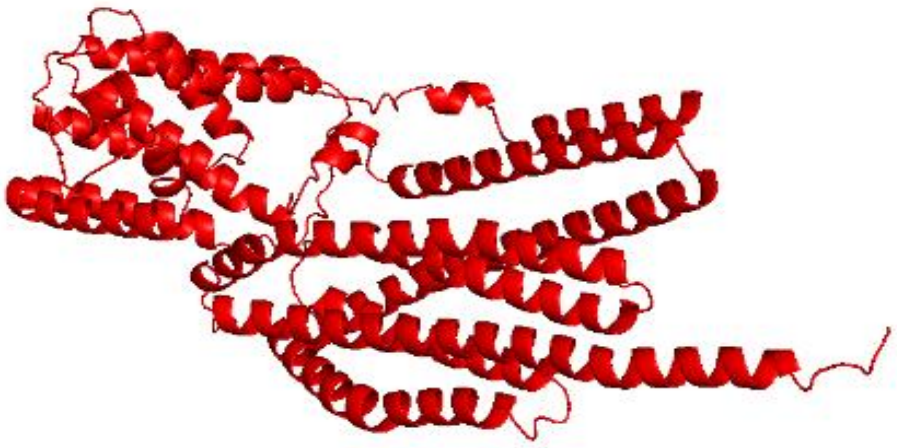

Fig (1): Protein structure of Cagβ.

ISSN No. 2321-2705 | DOI: 10.51244/IJRSI |Volume XIII Issue VII July 2026

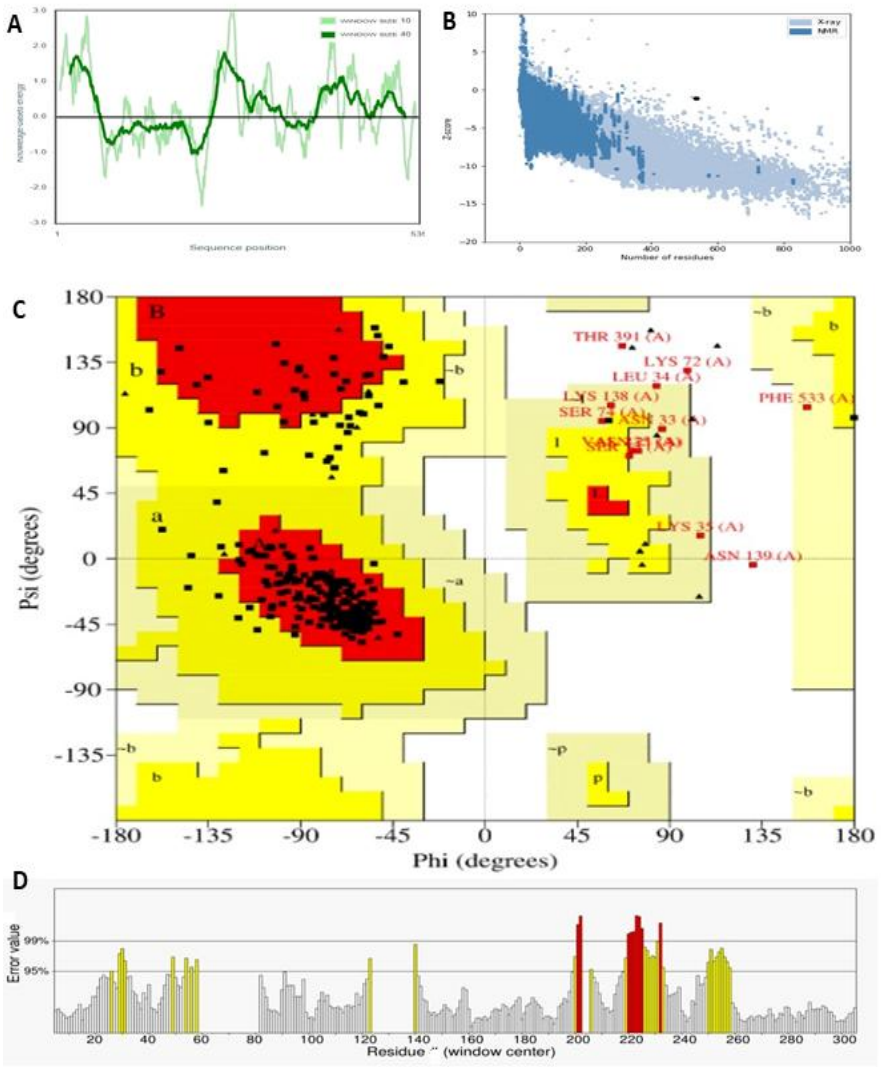

Fig (2): (A) ProSA energy plot for modelled Cagβ structure, (B) ProSA Z-score plot (C) Ramachandran plot for modelled Cagβ structure, (D) ERRAT plot shows modelled Cagβ structure.

Binding Pocket detection

The binding sites prediction of Cagβ protein resulted in the form of four pockets. The first binding pocket has the highest number of amino acids (Fig. 3, Table-1) which are mainly from catalytic domain.

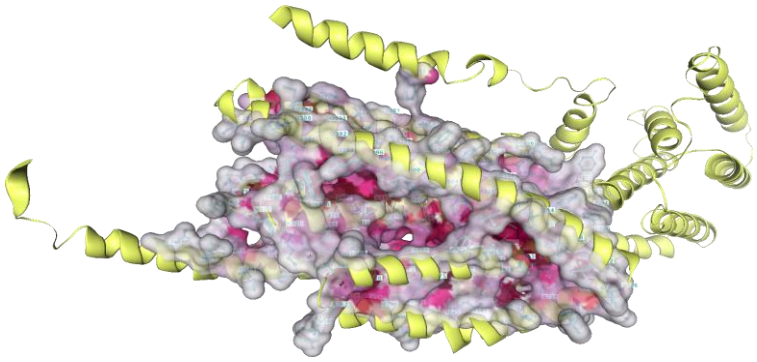

Fig (3): The ligand binding 1st pocket of Cagβ protein.

Among the predicted pockets, pocket 1 was found to be the best as it was always the largest and deepest cavity found on the protein. A total volume of 34,954 Å^3 with its spatial dimensions defined at a size of 30 by 30 by 30 along the X, Y, and Z axis, respectively. The central coordinates were positioned in -9.3 (X), -1.6 (Y), and 4.7 (Z) to accurately focus on the primary binding site.

ISSN No. 2321-2705 | DOI: 10.51244/IJRSI |Volume XIII Issue VII July 2026

TABLE-1: Binding Pocket 1 Residue Composition

Pocket 1	ILE458 THR343 MET423 SER403 GLY368 ALA440 ARG352 ALA453 LEU336 TRP418 GLY447 GLU496 GLU492 SER412 ALA323 SER480 VAL406 THR504 PHE446 MET516 ASN433 ASN432 ASN329 PHE268 ILE464 PHE260 PHE263 ILE266 THR483 ALA450 PHE380 ILE501 GLY404 VAL331 LEU340 GLY291 LEU416 VAL339 LEU348 LEU413 ALA298 PHE377 LYS270 LEU338 VAL438 GLN245 VAL236 VAL235 ALA372 ALA399 ILE282 PHE419 PHE251 VAL300 GLY246 TYR286 PHE490 SER390 SER461 THR493 GLU285 ASP512 ALA500 ASN237 GLN330 SER315 SER253 LEU449 SER497 LEU332 ILE347 PHE308 ALA479 ILE505 LEU230 PHE407 ALA362 PHE402 SER267 ILE482 GLY234 ILE486 SER476 THR391 ASN466 VAL509 ASN468 LEU472 ARG515 VAL502 VAL354 LEU249 VAL351 ILE379 LEU294 PHE302 VAL358 GLY489 ILE318 TYR305 PHE430 ILE314 GLU519 PHE435 VAL264 LEU444 PRO396 GLY400 ALA401 LYS420 ILE256 SER375 LYS424 ILE494 ILE398 GLY292 VAL290 THR384 LEU397 LEU311 ILE405 GLN465 PHE326 ILE409 LEU255 TYR312 TYR316 TYR319 ALA304 ILE385 LEU451 ILE386 ALA410 PRO231 ILE389 TYR257 ARG388 THR293 SER508 PRO408 TRP429 ASP240 ARG288 MET381 MET387 ILE414 PHE333 MET511 TRP334 GLY309 PRO239 PHE355 MET287 TYR248 VAL383 PHE15 SER422 SER301 ASP417 GLY261 LYS296 SER507 VAL462 LEU271 PHE320 THR459 ASN455 ASN361 ASN360 ILE474 ILE428 ILE426 LYS395 LEU376 TYR233 LEU427 PHE289 LEU322 ILE443 MET297 ILE441 GLN382 VAL393 VAL392 VAL394 GLY373 LEU434 LEU437 GLY471 VAL498 ILE274 LEU365 GLN469 LEU439 LEU328 LEU369 ALA335 VAL252 VAL415 PHE454 VAL411 VAL259 ILE431 ASN425 THR457 ILE436 LEU366

Virtual screening

DrugRep server was used for virtual screening from the approved drug library. The server short listed 120 drugs according to their lowest binding energy affinity. Among 120 shortlisted drugs we chose top five ligands for further study. These 5 compounds have binding energy ranging from − 11.6 kcal/mol to − 11.0 kcal/mol. A greater negative score is better as it represents strong chemical connections and more stable fit (Oleg and Arthur J.).

Molecular docking

Shortlisted 5 compounds were chosen for the molecular docking studies for revalidating binding affinity score with the help of AutoDock Vina. These top identified drugs against the Cagβ significantly showed highest binding affinity score in docking study (Table 2).

ISSN No. 2321-2705 | DOI: 10.51244/IJRSI |Volume XIII Issue VII July 2026

TABLE-2: Molecular Docking and Binding Affinity Analysis of Screened Drug Candidates against Pocket 1

Sl. No.	Drug Bank ID	Common Name	Chemical Class	Disease Treating or Managing	Mechanism of Action	Screened Binding Affinity (kcal/mol)	Docking Binding Affinity Score (kcal/mol)
1	DB11581	Venetoclax	Phenylpiperazines / Sulfonamides	Chronic lymphocytic leukemia (CLL), Acute myeloid leukemia (AML)	BCL-2 inhibitor (induces apoptosis)	–11.6	-12.5
2	DB00210	Adapalene	Naphthoic acid derivatives (Retinoids)	Acne vulgaris	Retinoic acid receptor (RAR) agonist	–11.5	-11.3
3	DB01167	Itraconazole	Triazoles	Systemic fungal infections (Aspergillosis, Candidiasis)	Lanosterol 14α-demethylase (CYP51) inhibitor	–11.2	-10.8
4	DB01396	Digitoxin	Cardiac glycosides	Heart failure, Cardiac arrhythmias	Na^+/K^+-ATPase membrane pump inhibitor	–11.1	–11.4
5	DB15328	Ubrogepant	CGRP receptor antagonists	Acute migraine with or without aura	Calcitonin gene-related peptide (CGRP) receptor antagonist	–11.0	–12.0

Visualization

Post docking, visualization of the receptor- ligand interactions were showed in PyMOL (3.1.8) software. Predicted structures confirmed that Venetoclax fits securely with the primary binding cavity of the Cagβ protein. The PyMOL 3D interaction analysis highlighted the ligand and the target residues are represented in stick format. The interaction analysis reveals the detailed binding configurations and specific bond lengths for the top five ranked drug compounds against the target protein (Fig. 4). Venetoclax demonstrated the strongest binding profile, establishing multiple close interactions with SER 301 (at distances ranging from 1.7 to 2.7 Å), Met 297 (2.9 Å), Gly 309 (2.9 Å), and Leu 249 (2.7 Å). Adapalene ranked second, forming contact networks primarily with TYR 305 (2.5–2.9 Å) and Ser 301 (2.8–2.9 Å). Itraconazole secured the third position by engaging SER 301 at 2.9 Å, Arg 338 at 2.2 Å, and Ile 405 at 2.4 Å. Digitoxin ranked fourth, interacting with SER 301 (2.4, 2.9 Å), Phe 260 (2.4, 2.9 Å), Tyr 305 (2.5 Å), Tyr 312 (3.0 Å), and Ser 315 (2.4 Å). Finally, Ubrogepant placed fifth, displaying key interactions with SER 403 (2.2–2.7 Å), Met 297 (3.0 Å), Phe 308 (2.4, 2.7 Å), and Phe 260 (2.8 Å). The molecular analysis of Venetoclax further confirms its superior inhibitory drug. Venetoclax establishes a highly dense and stable interaction network with the SER 301 residue of the Cag β protein. The shortest interaction distance, reaching as low as 1.7 Å to 1.8 Å, forms the most secure binding pose than all drugs. This perfectly syncs with the highest binding affinity score of -11.6.

ISSN No. 2321-2705 | DOI: 10.51244/IJRSI |Volume XIII Issue VII July 2026

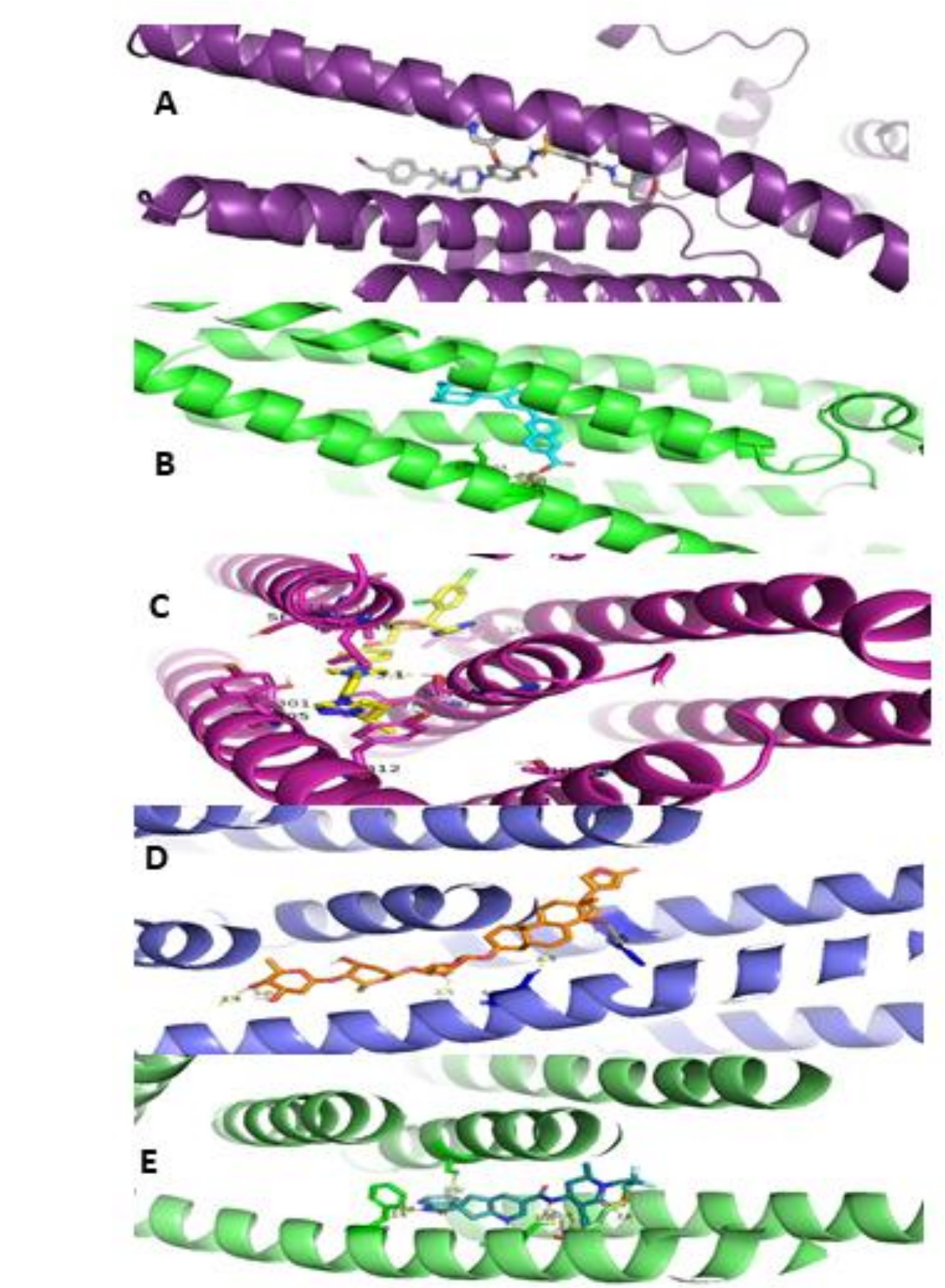

Fig (4): (A): Detailed view of the binding interaction between Venetoclax and the Cagβ receptor. **(B):** Visualization of the molecular interaction between Adapalene and the Cagβ receptor. **(C):** Visualization of the molecular interaction between Itraconazole and the Cagβ receptor. **(D):** Visualization of the molecular interaction between Digitoxin and the Cagβ receptor. **(E):** Visualization of the molecular interaction between Ubrogepant and the Cagβ receptor.

ISSN No. 2321-2705 | DOI: 10.51244/IJRSI |Volume XIII Issue VII July 2026

DISCUSSION

In absence of the crystal structure of Cagβ, we constructed comparative homology 3D model and validated the *Helicobacter pylori* T4SS coupling motor protein Cagβ; Cagβ utilizes ATP hydrolysis for the movement of CagA oncoprotein into the host cell. The structural validations were done using Ramachandran plot, ProSA and Errat that confirmed the stability and reliability of the predicted structure. The active site cavity of the protein was identified comprising the volume of 34,954 $Å^3$, which was further targeted for structure-based docking. The drug repurposing study short listed FDA approved 120 probable drugs among which five, Venetoclax, Adapalene, Itraconazole, Digitoxin & Ubrogepant were promising. Among the drugs, Venetoclax was the most promising lead. Venetoclax is an oral B-cell lymphoma-2(bcl-2) inhibitor, and approved in 2016 for hematic malignancies like chronic lymphocytic leukemia(CLL) and acute myeloid leukemia(AML) (Souers et al.). In our drug repurposing analysis, Venetoclax showed promising screening binding affinity and scored -11.6 kcal/mol and docking affinity of -12.5 kcal/mol in drug screening and Autodock Vina, respectively. The visualization in PyMOL revealed that Venetoclax forms tight, stable interaction anchoring to key residues Ser301 with short bond distanced from 1.7 to 2.7 Å and many additional contacts with Met297, Gly309 and Leu249. Venetoclax is predicted to hinder the ATP-driven motor activity of Cagβ, blocking the movement of CagA oncoprotein into the host cell. In future, the *in vitro* and *in vivo* lab validation is required to confirm its inhibition and biological efficacy against *H. pylori*.

CONCLUSION

From the above analysis, it is clearly concluded that Venetoclax may bind to the active site of the Cagβ and halt the energy dependent process of secretion machinery, effectively locking it in an inactive state. Consequently, preventing the movement of the oncoprotein CagA into the host gastric cells.

By disrupting this key step of *H. pylori* pathogenesis, Venetoclax has the potential to reduce the downstream inflammatory signalling and minimise the long-term risk of gastric cancer. As this approach specifically targets a virulence factor rather than general bacterial survival, it offers a highly powerful therapeutic drug that may reduce resistance and minimise disruption in host cell. More laboratory and clinical tests are needed to prove that venetoclax is a safe and effective treatment for *H. pylori* infections.

ACKNOWLEDGEMENTS

TS would like to acknowledge the Faculty Research Grant and RUSA Grant at University of Kalyani for the funding necessary for the research work.

Declaration of competing interest

The Authors declare no conflicts of interest

REFERENCE

1. Bateman, Alex, et al. “UniProt: The Universal Protein Knowledgebase in 2023.” *Nucleic Acids Research*, vol. 51, no. D1, 2023, https://doi.org/10.1093/nar/gkac1052.
2. Benkert, Pascal, et al. “Toward the Estimation of the Absolute Quality of Individual Protein Structure Models.” *Bioinformatics*, vol. 27, no. 3, 2011, https://doi.org/10.1093/bioinformatics/btq662.
3. Bissantz, Caterina, et al. “A Medicinal Chemist’s Guide to Molecular Interactions.” *Journal of Medicinal Chemistry*, vol. 53, no. 14, 2010, https://doi.org/10.1021/jm100112j.
4. Bowie, James U., et al. “A Method to Identify Protein Sequences That Fold into a Known Three-Dimensional Structure.” *Science*, vol. 253, no. 5016, 1991, https://doi.org/10.1126/science.1853201.
5. Colovos, Chris, and Todd O. Yeates. “Verification of Protein Structures: Patterns of Nonbonded Atomic Interactions.” *Protein Science*, 1993, https://doi.org/10.1002/pro.5560020916.
6. Correa, Pelayo, and Jean Marie Houghton. “Carcinogenesis of Helicobacter Pylori.” *Gastroenterology*, vol. 133, no. 2, 2007, https://doi.org/10.1053/j.gastro.2007.06.026.
7. DeLano, W. L. “The PyMOL Molecular Graphics System, Version 2.3.” *Schrödinger LLC*, 2020.
8. Gan, Jian hong, et al. “DrugRep: An Automatic Virtual Screening Server for Drug Repurposing.” *Acta*

Pharmacologica Sinica, 2023, https://doi.org/10.1038/s41401-022-00996-2.

9. Guevara, Bernardo, and Asha Gupta Cogdill. "Helicobacter Pylori: A Review of Current Diagnostic and Management Strategies." *Digestive Diseases and Sciences*, vol. 65, no. 7, 2020, https://doi.org/10.1007/s10620-020-06193-7.
10. Hooft, R. W. W., et al. "Errors in Protein Structures [3]." *Nature*, vol. 381, no. 6580, 1996, https://doi.org/10.1038/381272a0.
11. Hooi, James K. Y., et al. "Global Prevalence of Helicobacter Pylori Infection: Systematic Review and Meta-Analysis." *Gastroenterology*, vol. 153, no. 2, 2017, https://doi.org/10.1053/j.gastro.2017.04.022.
12. IARC. "Schistosomes, Liver Flukes and Helicobacter Pylori." *Iarc Monographs on the Evaluation of Carcinogenic Risks To Humans*, vol. 61, 1994.
13. Oleg, Trott, and Olson Arthur J. "AutoDock Vina: Improving the Speed and Accuracy of Docking with a New Scoring Function, Efficient Optimization, and Multithreading." *Journal of Computational Chemistry*, 2010, https://doi.org/10.1002/jcc.
14. Ramachandran, G. N., et al. "Stereochemistry of Polypeptide Chain Configurations." *Journal of Molecular Biology*, vol. 7, no. 1, 1963, https://doi.org/10.1016/S0022-2836(63)80023-6.
15. Souers, Andrew J., et al. "ABT-199, a Potent and Selective BCL-2 Inhibitor, Achieves Antitumor Activity While Sparing Platelets." *Nature Medicine*, vol. 19, no. 2, 2013, https://doi.org/10.1038/nm.3048.
16. Sung, Hyuna, et al. "Global Cancer Statistics 2020: GLOBOCAN Estimates of Incidence and Mortality Worldwide for 36 Cancers in 185 Countries." *CA: A Cancer Journal for Clinicians*, vol. 71, no. 3, 2021, https://doi.org/10.3322/caac.21660.
17. Tegtmeyer, Nicole, et al. "Role of the Cag-Pathogenicity Island Encoded Type IV Secretion System in Helicobacter Pylori Pathogenesis." *FEBS Journal*, vol. 278, no. 8, 2011, https://doi.org/10.1111/j.1742-4658.2011.08035.x.
18. Tohidpour, Abolghasem. "CagA-Mediated Pathogenesis of Helicobacter Pylori." *Microbial Pathogenesis*, vol. 93, 2016, https://doi.org/10.1016/j.micpath.2016.01.005.
19. Waterhouse, Andrew, et al. "SWISS-MODEL: Homology Modelling of Protein Structures and Complexes." *Nucleic Acids Research*, 2018, https://doi.org/10.1093/nar/gky427.
20. Wiederstein, Markus, and Manfred J. Sippl. "ProSA-Web: Interactive Web Service for the Recognition of Errors in Three-Dimensional Structures of Proteins." *Nucleic Acids Research*, 2007, https://doi.org/10.1093/nar/gkm290.
21. Wu, Xiuling, et al. "Mechanism of Regulation of the Helicobacter Pylori Cagβ ATPase by CagZ." *Nature Communications* , vol. 14, no. 1, 2023, https://doi.org/10.1038/s41467-023-36218-4.